YTUP

Journal of Thermal Engineering

https://jten.yildiz.edu.tr/

https://doi.org/10.47481/jten.0008

RESEARCH ARTICLE

Bio-inspired optimization of fuselage design for enhanced aerodynamic efficiency

Mohamed Arif Rajmohamed[1,*], Rohit Madugula[2], Kiranpreet Kaur Lotey[3], Khushi Agarwal[4]

[1]Department of Aerospace Engineering, College of Engineering and Technology, SRM Institute of Science and Technology, Kattankulathur, Chengalpattu District, Tamil Nadu, 603203, India
[2]Department of Aerospace Engineering, College of Engineering and Technology, SRM Institute of Science and Technology, Kattankulathur, Chengalpattu District, Tamil Nadu, 603203, India
[3]Masters Student, Aerospace Engineering, University of Texas at Arlington, Arlington, TX 76019, U.S.A.
[4]Department of Aerospace Engineering, College of Engineering and Technology, SRM Institute of Science and Technology, Kattankulathur, Chengalpattu District, Tamil Nadu, 603203, India

Abstract

The fuselage generates drag, contributing to the airplane's overall drag. To enhance aerodynamic efficiency and minimize fuel consumption, fuselage drag must be reduced. This study considers the implementation of a novel bio-inspired design modification to improve flow control and reduce drag on the fuselage and the aircraft. The fuselage was optimized by modifying the nose and body profiles inspired by marine creatures. The three-dimensional computational analysis was conducted on several modified fuselage configurations. The studies revealed that alterations made to the nose and the front section of the fuselage were ineffective, as these modifications affected only the nose and not the entire length of the fuselage. Modifying the flat upper surface of the fuselage into a curved profile using a NACA symmetric airfoil series resulted in improved flow acceleration and an extended low-pressure region. These modifications led to a maximum reduction in drag coefficient of 25% and a maximum increase in lift coefficient of 81%. The increased area resulting from the curvature of the upper surface can efficiently provide additional luggage storage, crew rest space, and greater passenger cabin capacity.

Keywords: Drag reduction; bio-inspired design; flow simulation; fuselage nose profile

Cite this article as: Rajmohamed, M. A., Madugula, R., Lotey, K. K., & Agarwal, K. (2026). Bio-inspired optimization of fuselage design for enhanced aerodynamic efficiency. Journal of Thermal Engineering, 12(3), 2–9. https://doi.org/10.47481/jten.0008

1. Introduction

Drag is the aerodynamic force that opposes an airplane's motion through the air. The drag experienced by an aircraft includes profile, induced, and parasitic drag As air accelerates around the fuselage, the pressure along its sides decreases. The pressure may continue to decrease along the midsection, depending on the shape. As the flow moves away from the surface, pressure drag may increase because of the formation of a turbulent wake. Factors affecting fuselage drag include its shape and size, surface roughness, and other characteristics. And comprehending and reducing fuselage drag is crucial for enhancing the aircraft's fuel efficiency and overall performance [1]. The most commonly used methods to reduce the fuselage drag are active and passive flow control. In those cases, passive flow-control methods such as laminar flow control (LFC), suction, oscillatory motions, riblets, vortex drag reduction, and alternative configurations such as span loaders and strut-braced wings, significantly reduce drag. The laminar flow control (LFC) on the fuselage shows the drag reductions for the fuselage by delaying boundary layer transition [2,3]. A ramp attached at the rear of the cargo aircraft decreases the drag coefficient by 8% [4]. The dual-use aft cargo ramp and micro vanes reduced the drag, resulting in fuel savings of up to 30 gallons per flight hour [5]. The drag-reduction potential of the finlet and the microvane is equal for different counts on both sides of the fuselage. And both designs showed a 1% fuel savings [6-8] and discussed the effect of riblets on skin friction reduction on fuselage. The riblets reduced the skin friction drag by 6.5%.

*Corresponding Author
E-mail Adress: arif.aero21@gmail.com

Submitted: 5 December 2025; **Accepted:** 11 January 2025

This paper was recommended for publication in revised form by Editorin-Chief Ahmet Selim Dalkılıç

The beaver-tail strakes attached to a fuselage reduced drag, increased longitudinal stability, and had a negligible effect on lateral stability. It was predicted that the drag reduction results in annual fuel savings of about 35.5 million pounds [9]. The non-axisymmetric fuselage design is reducing drag while maintaining low sonic-boom characteristics [10]. A decrease in the nose-shape factor reduces the fuselage drag coefficient. The tail section with a larger upsweep angle and a longer tail increases the drag coefficient [11]. The hood, tail fairing, and windshield also play key roles in drag generation. It should be varied carefully to achieve a more streamlined appearance. Windshield drag can account for 15% of an airplane's total drag. The longitudinal profile of a windscreen is more important than its transverse profile. It is also found that the recessed windows, telescoping hood steps, and retaining strips are affecting drag [12]. The conventional UAV fuselage optimized using the spline shows a reduction in the drag of up to 50% [13]. The airfoil-shaped UAV fuselage showed an increase in the L/D of up to 8.37% [14]. The geometry of the A320 fuselage was studied and modified to produce a fuselage that does not require a tailplane. The optimized designs increased the pressure difference between the top and bottom surfaces of the fuselage, making the fuselage a lifting body [15]. The optimized A310 fuselage has improved in the fineness ratio, which contributed to the reduction of the drag coefficient (4.8%), lowered take-off and landing distance, and enhanced rate of climb [16]. The variation in fuselage diameter didn't affect the lift coefficient but increased the drag coefficient due to increased skin-friction drag [17]. The aerodynamic and structural properties of the twin-fuselage configuration, as well as its advantages, have been discussed. Rearranging the power plant redistributes the weight, resulting in structural improvements such as reduced bending loads. Additionally, the optimization of the wing design and increased aspect ratio have increased aerodynamic efficiency [18].

The blended-wing body integrates wings and fuselage into a unified structure. This design enhances aerodynamic efficiency by reducing drag and improving lift-to-drag ratios [19–24]. It offers potential benefits, such as increased fuel efficiency, reduced emissions, and greater payload capacity [25]. The design has attracted attention because it has the potential to meet stricter environmental regulations and to optimize the performance of future aircraft. Among active flow-control methods, estimates indicate that suction of air from slots in the forward fuselage can reduce fuselage skin friction by up to 10%. [26, 27]. The simultaneous shape optimization of both the fuselage and wing at the intersection region shows the 2% drag reduction [28]. The application of active flow control, using eight slots arranged in a U-shape around the flow separation lines, reduced fuselage drag: steady blowing at the rear ramp delayed flow separation by increasing the surface pressure acting on it, thus decreasing the overall fuselage drag by 35% compared to the base model. Additionally, unsteady blowing demonstrated a 26% reduction in drag [29]. The riblet valleys are filled with fluid, which acts as a lubricant and allows the flow to slip over the ribbed surfaces. Retention of fluids in transverse riblet surfaces reduces the drag [30]. The average drag reduction by riblet surfaces was found to be nearly 10% [31, 32]. At low speeds, riblets are more effective in controlling adverse pressure gradients [33, 34].

The aforementioned studies demonstrate the diverse alterations to the fuselage. Most studies include modifications to the windshield designs, incorporation of micro vanes, alterations in nose and tail sections, the Laminar flow control method, etc., to minimize the drag. In recent years, biomimicry has played a key role in the design optimization of vehicle aerodynamics. Bio-inspiration from cetaceans (dolphins, whales, and porpoises, which have streamlined bodies that enable faster, more efficient swimming) improves the aerodynamic design of aircraft because the Reynolds number associated with cetacean swimming corresponds to the range of aircraft speeds. Most existing bio-inspired studies investigate surface-roughness modifications inspired by marine animals' body textures (e.g., shark skin scales), but the fabrication and installation of such microstructures on existing aircraft are complex and yield a maximum drag reduction of only 10%. This study primarily focuses on applying the aerodynamic features of marine mammals, excluding skin texture, to the fuselage to minimize drag.

2. Methodology

This study aims to optimize the fuselage of the commercial airliner Airbus A320 through a bioinspired design approach. This model is the most widely used aircraft among commercial airlines because its wide single aisle provides comfortable seating for 120–244 passengers. Figure 1 shows the reference fuselage and its dimensions. The scaled-down model has a length of 37.57 mm and a height of 4.12 mm. The fuselage profile design was further modified, drawing inspiration from cetaceans, to assess drag reduction. Most marine species exhibited elongated vertical body profiles. This inspired the current design, in which the fuselage's flat-top profile was changed to a curved profile. Marine animals are a more suitable source of bio-inspiration for aircraft optimization than birds, particularly with respect to Reynolds number. Large marine species such as dolphins, whales, and tunas operate in flow regimes (10^6–10^8) that closely match those of aircraft, in which inertial forces dominate and turbulent boundary-layer behavior is critical. In contrast, birds typically fly at lower Reynolds numbers, making their feather-based aerodynamic strategies less scalable to full-size aircraft.

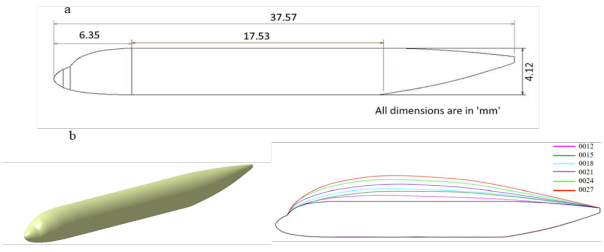

Figure 1. a) Side view & b) Isometric view of the reference model (A320 fuselage) (Left) and Fuselage body profile modification with airfoil design

The NACA symmetric airfoils of different thicknesses (NACA0012, NACA0015, NACA0018, NACA0021, NACA0024, and NACA0027) were used to form the curved top profile of the fuselage, as mentioned in Figure 1. The airfoil with a thickness greater than 12% was used to achieve sufficient curvature on the upper surface of the fuselage profile. The height of the fuselage increased by approximately 21%, 29%, 36%, 46%, 61%, and 72% for the NACA0012, NACA0015, NACA0018, NACA0021, NACA0024, and NACA0027 airfoils, respectively. These modifications led to an increase in the cross-sectional area of the fuselage. The space resulting from an increase in fuselage height can be used for additional baggage or cargo space, or the fuselage can be converted into a double-deck aircraft in the case of the NACA 0027 airfoil.

2.1. Computational domain

For computational analysis, a multi-block C-grid domain was created to refine the mesh, as shown in Figure 2(a, b). A C-grid domain was created around the fuselage, extending to 10 times the model length. The cut-cell technique was used to create structured meshes in most regions.} Different element sizes were defined for all subdomains. The inflation layers were added to capture the near-wall effects on the reference fuselage. The steady-state subsonic pressure-based flow analysis was conducted using Ansys Fluent software. SIMPLEC was selected as the solution method. The least-squares cell-based method was used to calculate the gradient of the variables. A second-order upwind method is used to compute the momentum, turbulent kinetic energy, and specific dissipation rate. The Default solution limits were used. The realizable k–ϵ model was used in the simulations because the fuselage model is a long bluff body. A velocity-inlet boundary condition of 90 m/s was applied at the inlet, and a pressure-outlet boundary condition of 0 Pa was applied at the outlet. The model's vertical side boundary is assumed to be symmetrical. The operating Reynolds number and Mach number of A320 aircraft at cruising altitude are Re = 2.318x10^8 and M = 0.78. Hence, the inlet velocity was set to 90 m/s for sea-level conditions to maintain the same Reynolds number.

A mesh independence study was conducted for the reference fuselage model (A320). The element size was reduced to 50% for each new case, yielding different total mesh element counts: 0.5 million, 0.7 million, 1 million, and 1.5 million elements. Figure 2(c) shows that the drag coefficient varies across different mesh elements. The changes in drag coefficient (Cd) after 1 million elements were negligible, approximately 1%. Hence, 1.5 million mesh elements were finalized for use in further analysis.

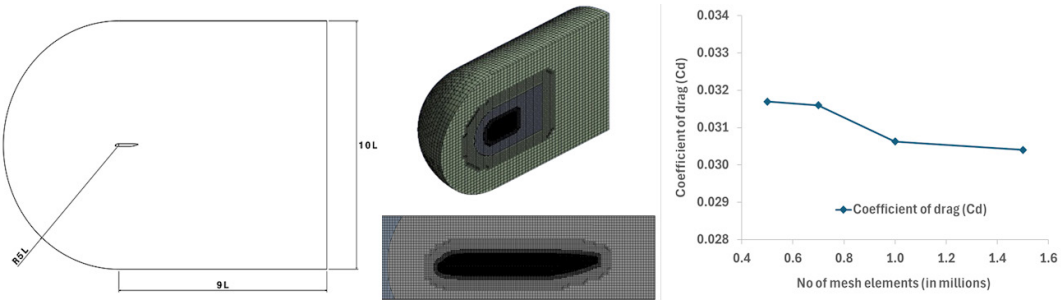

Figure 2. a) C-Grid Domain, **b)** Domain with Cut cell mesh (Top) and fine mesh around the fuselage body (bottom), and **c)** Mesh study for different mesh elements.

Table 1. Mesh independence study for different mesh elements

No of mesh elements (in millions)	0.5	0.7	1.0	1.5
Coefficient of drag (Cd)	0.0317	0.0316	0.0306	0.0304

3. Results and discussions

The subsonic flow analysis was carried out for the A320 fuselage model under cruising conditions. Modifications to the fuselage include changes to the nose and body profile. Aerodynamic parameters of the A320 fuselage, such as lift coefficient, drag coefficient, pressure, velocity, and wake regions, were compared with those of the modified fuselage designs, and the results are presented. Different contours and streamline patterns around the Airbus A320 fuselage are displayed in Figure 3. A flow-acceleration region is observed on the fuselage nose profile. The streamlines show the high-pressure region on the stepped profile of the nose section. Deceleration of the

flow on the fuselage surface increases the size of the wake region. This, in turn, affects the Cl (-0.0136) and Cd (0.0340) coefficients of the A320 fuselage. Further designs were considered to reduce aerodynamic drag by eliminating the high-pressure region and accelerating flow over the fuselage surface.

3.1. Aerodynamic properties of the fuselage with nose modifications

Fuselage nose modifications inspired by various cetacean species were analyzed. The modifications include a blunt nose profile, increased nose length, and upward and downward nose deflections. The results for the above-mentioned cases are summarized below.

The variations in the streamline patterns, vorticity, and velocity contours around the nose profiles of fuselages with different nose lengths, relative to the fuselage are displayed in Figure 3. Nose-profile alterations did not lead to any reduction in coefficient of drag (Cd) values. The modification, blunt-nose profile (B), has a pressure distribution similar to that around the stepped profile of the nose section. The elongated nose profile (C) also exhibits a similar pressure distribution, with a slight decrease in the maximum pressure at the stepped section of the nose. All modifications exhibit a low-pressure region on the fuselage aft of the nose section, indicating a flow-acceleration zone along the body surface.

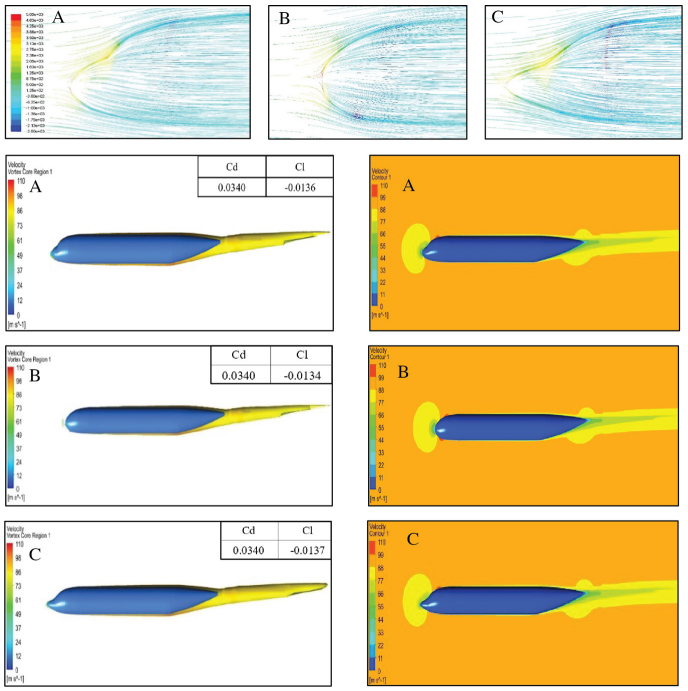

Figure 3. Streamline pattern (colour: pressure), Vorticity and Velocity contours of **(A)** Base model, **(B)** Blunt nose profile, **(C)** Elongated nose.

The streamline patterns, vorticity, and velocity contours of the reference model with nose-profile deflections are displayed in Figure 4. The aim was to accelerate the flow near the nose by modifying the nose section. Due to the deflection, the maximum pressure on the stepped section increased, leading to a higher Cd value. The velocity contours of the fuselage with nose modifications resemble those of the A320 fuselage. The variation in the profiles does not generate a sufficient pressure difference to accelerate the flow and reduce the wake region.

Figure 4 shows no apparent reduction in the wake region despite multiple modifications to the fuselage nose section. Figure 5 reveals that nose modifications, including blunting and nose deflections, do not reduce the Cd value. These designs did not accelerate the flow near the nose section. The Cl values for the above modifications remained unchanged because the designs failed to improve the aerodynamic characteristics of the fuselages. These modifications only affect the flow properties near the nose section, compared with those of the long, slender fuselage. Figure 5 shows that changes in the nose profile did not reduce fuselage aerodynamic drag.

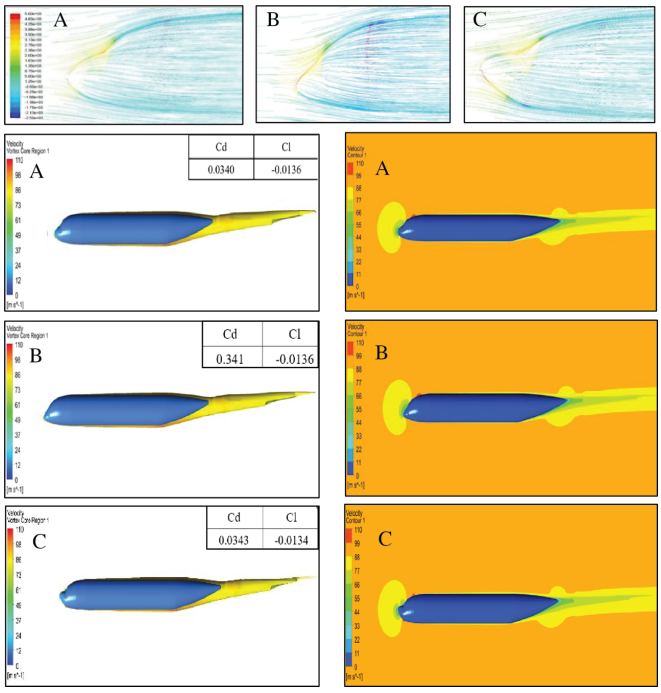

Figure 4. Streamline pattern (colour: pressure), Vorticity and Velocity contours of **(A)** Base model, **(B)** Nose deflected downwards, **(C)** Nose deflected upwards

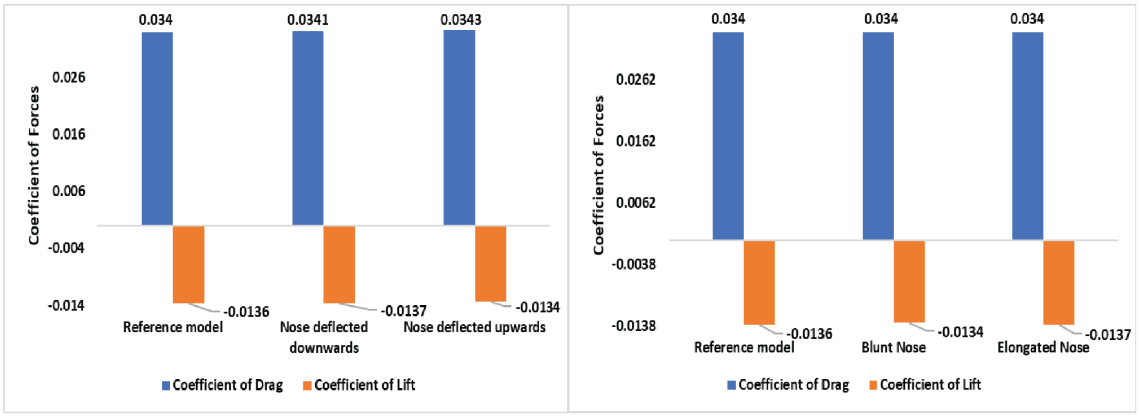

Figure 5. Variation of Cl and Cd for different nose modifications compared to base model.

3.1. Aerodynamic properties of fuselage body profile modification

The modifications to the A320 fuselage profile were conducted using airfoil designs that included NACA0012, NACA0015, NACA0018, NACA0021, NACA0024, and NACA0027 profiles. To minimize the aerodynamic drag on the fuselage, the body was streamlined through modifications. Initial modifications were made to the fuselage of the existing aircraft without affecting its cross-sectional area. A parametric study was conducted on profiles with increased cross-sectional area to assess the variation in Cl, Cd, and L/D; the results are shown in Figures 6 and 7.

The initial modification was primarily aimed at reducing the fuselage drag of the current A320. The current A320 fuselage was modified to incorporate the NACA0012 body profile without altering its cross-sectional area, as shown in Figure 6. This streamlined shape has reduced the Cd by accelerating flow over the fuselage surface. This can be observed in the pressure contours; the extension of the low-pressure region on the fuselage surface helps the flow accelerate. Variations in Cl and Cd are observed between the A320 fuselage and the optimized model in Figure 7. The streamlined design decreases the drag coefficient by 7% and increases the lift coefficient by 33% without varying the cross-sectional area of the fuselage. Further study involved varying the cross-sectional area of the A320 fuselage. Figure 8 shows low-pressure regions. Extended low-pressure regions on the fuselage have increased relative to those on the A320 fuselage.

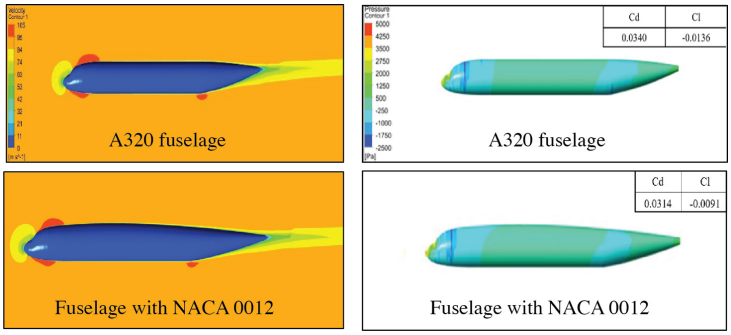

Figure 6. Velocity and Pressure contour for the A320 fuselage, modified fuselage with NACA 0012 profile.

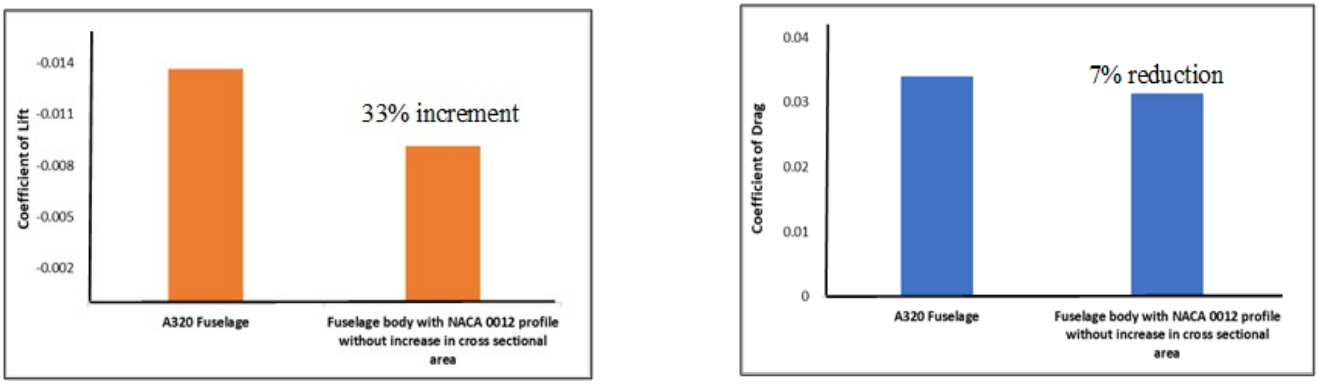

Figure 7. Variation of Cl and Cd for base fuselage and modified fuselage with NACA 0012 profile

The modified fuselage body profile, which features an airfoil that transitions from 0012 to 0027, has produced an extended low-pressure region owing to an increase in cross-sectional area. Thus, flow acceleration on the fuselage improved. As a result, the relatively high-pressure regions on the fuselages of the modified designs were significantly reduced. This reduces the aerodynamic drag of the modified design as the flow accelerates over the surface of the fuselage. Thus, the lift force increases while the overall drag of the fuselage decreases. Fuselage designs with the NACA 0012 profile and with increased cross-sectional area incorporating NACA 0021 and NACA 0027 design modifications have been finalized based on the CFD simulations. The Cl and Cd values have been plotted and compared across the modified designs.

Figure 9 shows an increase in the lift coefficient and a reduction in the drag coefficient of the modified fuselage. An increase in cross-sectional area significantly improved the Cl and Cd values. Increasing the cross-sectional area beyond 21% of the thickness limited reductions in Cd values. The decrease in Cd for the fuselage with the 0021 profile is small. Figure 10 shows that two additional modifications may improve the L/D ratio. These two design models have been further studied and compared with the reference fuselage. The following comparisons can be used to differentiate between profiles 0021 and 0027.

The modified fuselage profiles have been compared with the reference fuselage profile. The modified fuselage body profiles have an extended low-pressure region with an increased cross-sectional area. Figure 8 illustrates the variation in the extended low-pressure regions among the finalized fuselage designs. The extent of the low-pressure region on the body increases with cross-sectional area.

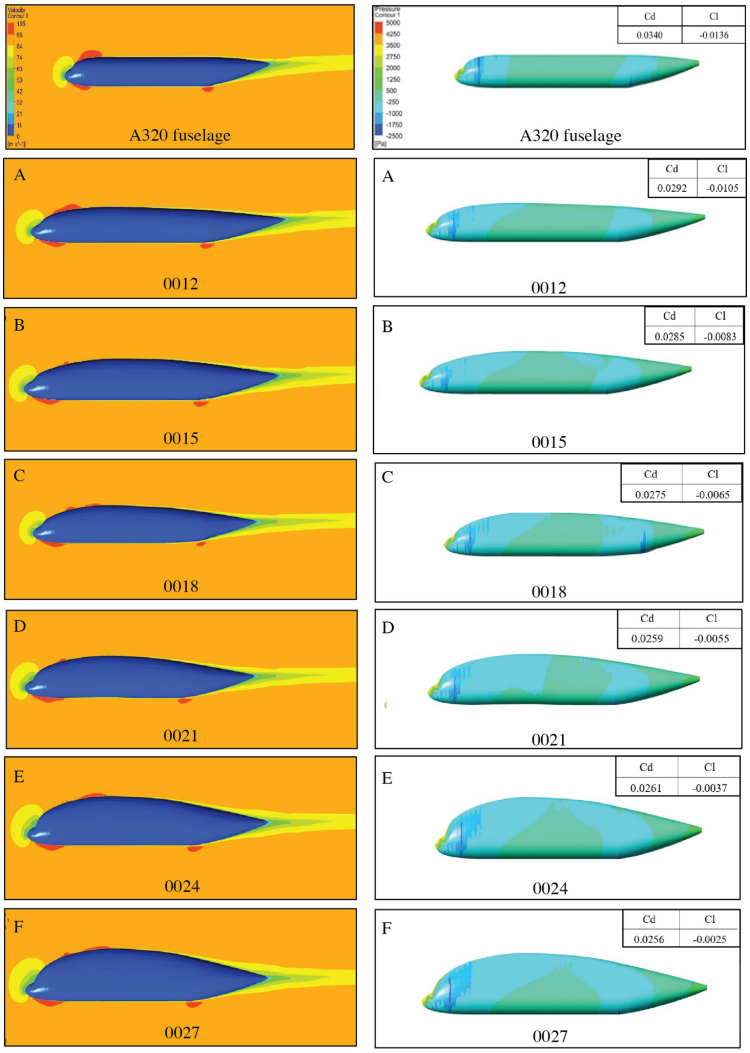

Figure 8. Velocity and Pressure contours for fuselage with modified body profile using airfoil design with(A)NACA 0012,(B)NACA 0015,**(C)**NACA 0018,**(D)**NACA 0021,**(E)**NACA 0024 and**(F)**NACA 0027

The additional area of these profiles can be utilized for storage space, either for cargo or to accommodate a crew rest area. The increase in Cl and the decrease in Cd for the modified profiles and the A320 fuselage are shown in Figure 10. A maximum 81% increase in lift force can be achieved using the NACA 0027 profile. Similarly, a maximum decrease of 25% in the drag force can be observed. All the finalized profiles are more streamlined than the A320 fuselage, resulting in a greater reduction in drag force. Hence, three designs have been finalized. The NACA 0012 airfoil design can be applied to the existing A320 fuselage without increasing the cross-sectional area. Other increased-thickness profiles can be used on cargo or double-decker aircraft.

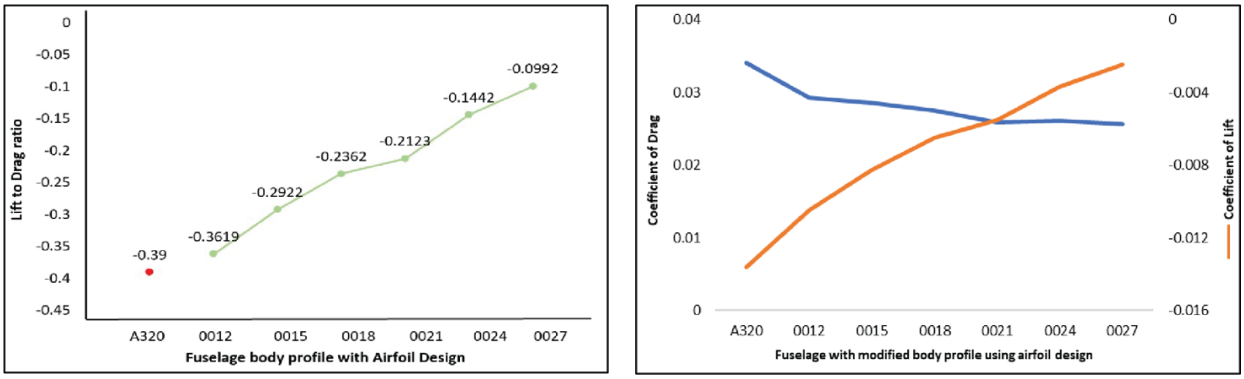

Figure 9. Variation of Cd, Cl, and L/D of different fuselage body profile modification

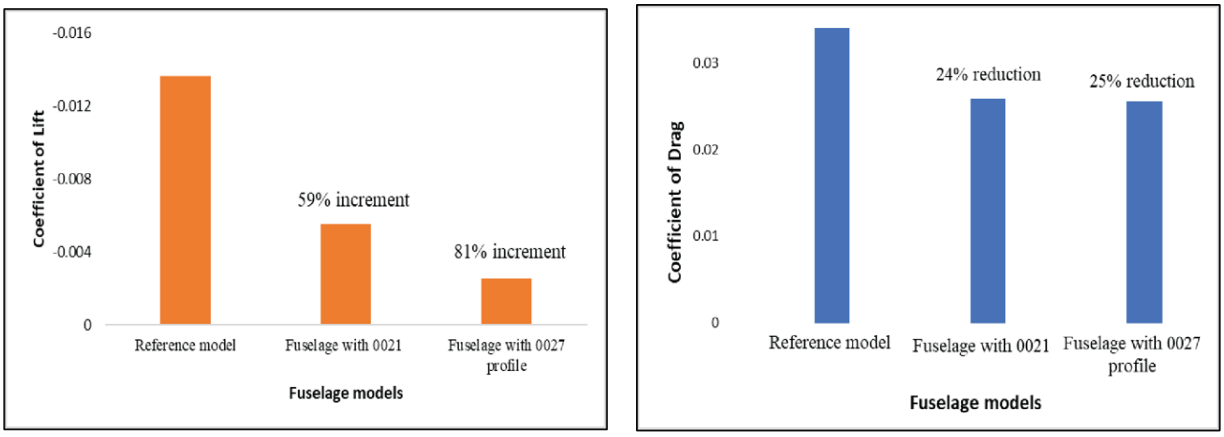

Figure 10. Percentage of change in Cl and Cd for the A320 and modified fuselage models

Table 2. Aerodynamic forces coefficients of Base fuselage with and without modification using NACA airfoil profiles.

S.No	Design Cases	Cd	Cl
1	Base Fuselage	0.0341	-0.014
2	Fuselage body profile modified using NACA 0012	0.0292	-0.011
3	Fuselage body profile modified using NACA 0015	0.0286	-0.008
4	Fuselage body profile modified using NACA 0018	*0.0276*	*-0.007*
5	Fuselage body profile modified using NACA 0021	0.0261	-0.006
6	Fuselage body profile modified using NACA 0024	*0.0260*	*-0.004*
7	Fuselage body profile modified using NACA 0027	0.0256	-0.003

4. Conclusion

A computational analysis was conducted on the fuselage, incorporating bio-inspired nose and body modifications. The modifications include changes to the nose and body profiles of the fuselage. The aerodynamic characteristics of the modified fuselage were compared, and the outcomes are presented below.

Bio-inspired nose modifications on the fuselage affected the flow properties only on the nose and not on the longer fuselage body. Fuselage profile modifications using airfoil shapes improve aerodynamic performance by increasing lift and reducing drag. The fuselage profile modification using the NACA 0012 airfoil, without increasing cross-sectional area, achieves the optimal drag reduction by reducing the drag coefficient by up to 7%. Increasing the airfoil thickness enhances flow acceleration and extends the low-pressure region over the fuselage, thereby increasing lift by a maximum of81% and decreasing drag by a maximum of 25%.

Observations indicate that increasing the fuselage profile thickness beyond 21% does not produce further reductions in drag because of the corresponding increase in cross-sectional area. The modified fuselage body profile with a NACA 0021 airfoil increases the lift by 59% and decreases the drag by 24%; additionally, the extra space can be used for cargo or baggage. Because the additional fuselage volume is used for cargo, it does not require pressurization, thereby reducing structural complexity and fabrication costs. The modified fuselage with the NACA 0027 airfoil increases lift by 81% and decreases drag by 25% and provides extra space that can be used as a passenger cabin. These modifications, which increase the curvature of the body profile, can be applied to fuselage designs for double-decker aircraft. It offers greater internal volume but necessitates pressurization and more complex structural integration, which increases manufacturing complexity and cost.

In future studies, passenger aircraft fuselage designs may be modified using different NACA airfoil profiles to identify the optimal design applicable to common fuselage configurations. Additionally, the simulation can be used to determine the effect of body profile modifications across different Mach number ranges, up to critical Mach numbers. Further analysis is required of the additional space, weight, and structural aspects of the modified fuselage design. Finally, the optimum design can be analyzed experimentally to validate the simulation results.

Copyright and permission statement

References

[1] Lai HC, & Kamaruddin NM. (2018), 'Effect of fuselage diameter on aerodynamic characteristics for straight wing at low and high aspect ratio', Int. Conference on Aerospace and Mechanical Engineering, Vol. 370.

[2] Beck N, Landa T, Seitz A, Boermans L, Liu Y, & Radespiel R. (2018), 'Drag reduction by laminar flow control', Energies, 11(1), 252.

[3] Dodbele SS, Van Dam CP, Vijgen PMHW, & Holmes BJ. (1987), 'Shaping of airplane fuselages for minimum drag', Journal of Aircraft, 24(5), 298–304.

[4] Mirzaei M, Karimi MH, & Vaziri MA (2012), 'An investigation of a tactical cargo aircraft aft body drag reduction based on CFD analysis and wind tunnel tests', Aerospace Science and Technology, 23(1), 263–269.

[5] Smith BR, Yagle P J, & Hooker JR. (2013), 'Reduction of AFT fuselage drag on the C-130 using microvanes', 51st AIAA Aerospace Sciences Meeting Including the New Horizons Forum and Aerospace Exposition.

[6] Lorang T, and John C, (2017), 'C-17A Globemaster III Aft Fuselage Drag Reduction Flight Demonstrations', AIAA Flight Testing Conference, p. 3653. 2017.

[7] Walsh MJ. (1986), 'Riblets for aircraft skin-friction reduction', Langley Symposium on Aerodynamics, Volume 1. 19880005573.

[8] Walsh M, Sellers IIIW, & McGinley C. (1988), 'Riblet drag reduction at flight conditions', 6th Applied Aerodynamics Conference. 19880053537.

[9] Pinsky HG, Gray M, Welch MD, & Yechout TR. (2009), 'Evaluation of the Drag Reduction Potential and Static Stability Changes of C-130 Aft Body Strakes', Aerospace Research Central.

[10] Makino Y, Suzuki K, Noguchi M, & Yoshida K. (2003), 'Nonaxisymmetrical fuselage shape modification for drag reduction of Low-Sonic-Boom airplane', AIAA Journal, 41(8), 1413–1420.

[11] Nicolosi F, Danilo C, Vecchia PD, & Cusati V. (2015), 'Fuselage Aerodynamic Drag Prediction Method by CFD', ResearchGate, 2015.

[12] Robinson RG, & Delano JB. (1942), 'An investigation of the drag of windshields in the 8-foot High-Speed wind tunnel', Langley Memorial Aeronautical Laboratory (730).

[13] Srinavasa V, Sridhara S, Nagappa GA, & Biradar BA. (2016), 'Estimation and reduction of drag in fuselage of solar powered UAV', 2016 IEEE Aerospace Conference, Big Sky, MT, USA.

[14] Alam GMJ, Mamun M, Ali MAT, Islam MQ, & Islam AKMS. (2013), 'Investigation of the aerodynamic characteristics of an aerofoil shaped fuselage UAV model', 10th Int. conf. on Mechanical Engg.

[15] Odendaal DU, Smith L, Craig K J, & Sanders DS. (2024), 'Computational investigation of the aerodynamic performance of an optimised alternative fuselage shape', Aircraft Engineering and Aerospace Technology, Volume 96, Issue 11.

[16] Dhara A, Majumder A, Kumar NE, Dhanunjay M, Dhanumjaya LT, & Jeyan JVML. (2024), 'Design optimization to minimize wake of wide-body transport aircraft', Journal of Engineering Research, Volume 12.

[17] Lutz T, & Wagner S. (1998), 'Drag reduction and shape optimization of Airship bodies', Journal of Aircraft, 35(3), 345–351.

[18] Vedernikov YV, Chepiga VE, Maslakov VP, Kuklev EA, & Gusev VG. (2017), 'Configuration of the Medium-Haul Twin-Fuselage Passenger Aircraft', International Journal of Applied Engineering Research, Volume 12.

[19] Liebeck RH. (2004). Design of the blended wing body subsonic transport. Journal of Aircraft, 41(1), 10–25. https://doi.org/10.2514/1.9084

[20] Qin N, Vavalle A, Le Moigne A, Laban M, Hackett K, & Weinerfelt P. (2004). Aerodynamic considerations of blended wing body aircraft. Progress in Aerospace Sciences, 40(6), 321–343. https://doi.org/10.1016/j.paerosci.2004.08.001

[21] Wang Y, Qin S, Xiang Y, Liu H. (2017). Interaction Mechanism of Vortex System Generated by Large Civil Aircraft Afterbody. Journal of Aeronautics, Astronautics and Aviation, Vol.49, No.1, pp.065 - 074 (2017) 65 https://doi.org/10.6125/16-1121-912

[22] Muta'ali ABA, Noryatim ANM, Nasir REM, Hamid AHA, & Mokhtar AS. (2024). Aerodynamics Analysis of a Boomerang Blended-Wing-Body Unmanned Aerial Vehicle using Different Numerical Simulation Tools. Journal of Aeronautics, Astronautics and Aviation, 56(1S), 319-331.

[23] Danial, Muhammad & Nasir, Rizal & Romli, Fairuz. (2024). Flight Performance Analysis of a Blended Wing-Body Unmanned Aerial Transport Vehicle. Journal of Aeronautics, Astronautics and Aviation. 243-256. 56(1). https://doi.org/10.6125/JoAAA.202403_56(1S).14

[24] Kroo, I. (1999). 'Aerodynamic concepts for future aircraft,' Fluid Dynamics Conference, Norfolk, VA, USA

[25] Dakka S & Johnson O. (2019). 'Aerodynamic Design and Exploration of a Blended Wing Body Aerodynamic Design and Exploration of a Blended Wing Body Aircraft at Subsonic Speed,' International Journal of Aviation, Aeronautics, and Aerospace, 6(5). https://doi.org/10.15394/ijaaa.2019.1411

[26] Reist, T. A., & Zingg, D. W. (2016). High-Fidelity aerodynamic shape optimization of a Lifting-Fuselage concept for regional aircraft. Journal of Aircraft, 54(3), 1085–1097. https://doi.org/10.2514/1.c033798

[27] Bushnell DM, (2003), 'Aircraft drag reduction—a review', Proceedings of the Institution of Mechanical Engineers, Part G: Journal of Aerospace Engineering, 217(1), 1–18.

[28] Matos, N. M. B., & Marta, A. C. (2025). Aerodynamic shape optimization of Wing–Fuselage intersection for minimum interference drag. Aerospace, 12(5), 369. https://doi.org/10.3390/aerospace12050369

[29] Schaeffler NW, Allan BG, Lienard C, & LePape A. (2010), 'Progress towards fuselage drag reduction via active flow control: a combined CFD and experimental effort', 36th European Rotorcraft Forum.

[30] Fu, Y., Yuan, C., & Bai, X. (2017). Marine drag reduction of shark skin inspired riblet surfaces. Biosurface and Biotribology, 3(1), 11–24. https://doi.org/10.1016/j.bsbt.2017.02.001

[31] Dean, B., & Bhushan, B. (2010). Shark-skin surfaces for fluid-drag reduction in turbulent flow: a review. Philosophical Transactions of the Royal Society a Mathematical Physical and Engineering Sciences, 368(1929), 4775–4806. https://doi.org/10.1098/rsta.2010.0201

[32] Pakatchian, M. R., Rocha, J., & Li, L. (2023). Advances in riblets design. Applied Sciences, 13(19), 10893. https://doi.org/10.3390/app131910893

[33] Viswanath, P. (2002). Aircraft viscous drag reduction using riblets. Progress in Aerospace Sciences, 38(6–7), 571–600. https://doi.org/10.1016/s0376-0421(02)00048-9

[34] Wang, D., & Liu, H. (2025). A novel aerodynamic drag-reduction mechanism using dolphin-inspired ultrasonic microvibrations. Scientific Reports, 15(1). https://doi.org/10.1038/s41598-025-98585-w